第25卷第6期
2006年12月

红外与毫米波学报
J. Infrared Millim. Waves

Vol. 25, No. 6
December, 2006

文章编号:1001-9014(2006)06-0401-04

ELECTRICAL TRANSPORT PROPERTIES OF $BiFeO_3$ THIN FILM

SUN Jing-Lan, LI Ya-Wei, LI Tian-Xin, LIN Tie, CHEN Jing, MENG Xiang-Jian, CHU Jun-Hao

(National Laboratory for Infrared Physics, Shanghai Institute of Technical Physics, Chinese Academy of Sciences Shanghai 200083, China)

Abstract: DC electrical transport properties of perovskite $BiFeO_3$ thin films were studied in the temperature range from 80K to 300K. The films with high or low resistance on $SrTiO_3$ substrates were prepared by a chemical solution deposition method from the same precursor solution at different aged time. For the low resistance samples, the voltage dependence of current is ohmic and temperature independent at low electric fields. At a medium strength of electric field, it behaves like a typical Schottky diode. For the high resistance samples it is found that electric carriers move along the grain boundaries of the films with an activation energy of 0.57eV at low electric field while the conduction mechanism can be described with the Frenkel-Poole model with an energy barrier of 0.12eV at higher electric fields, The measurable maximum values of remnant polarization are 2.6μC/cm² and 28.8μC/cm² at the temperature of 85K for the two kinds of samples, respectively.

Key words: biferroic film; electrical transportation; bismuth ferrate film

CLC number: 0482.4 **Document**: A

$BiFeO_3$ 薄膜中的电学输运性质

孙璟兰, 李亚巍, 李天信, 林 铁, 陈 静, 孟祥建, 褚君浩

(中国科学院上海技术物理研究所 红外物理国家重点实验室, 上海 200083)

摘要: 报道了铁酸铋薄膜样品在80K~300K温度范围直流电学输运性质的研究结果. 利用同一前驱体不同老化时间, 用化学溶液沉积法在钛酸锶衬底上制备出两种样品. 在低阻样品中, 低场下电流随电压变化遵从欧姆定律, 电阻不随温度变化; 而在中等强度外场下显示出肖特基二极管性质. 在高阻样品中, 低场下电流密度沿晶界分布, 输运中的势垒能级为0.57eV; 高场下电流的传输则遵从Frenkel-Poole模型, 相关势垒能级0.12eV. 低阻和高阻两种样品在85K温度下可测最大剩余极化分别为2.6μC/cm² 和28.8μC/cm².

关 键 词: 铁电铁磁薄膜; 电学输运; 铁酸铋薄膜

Introduction

Multiferroic materials possessing both ferroelectricity and ferromagnetism properties have attracted much attention because of their potential use in microelectronic devices in recent years. As a lead-free ferroelectrics materials, $BiFeO_3$ draws much interests not only for its biferroic nature but also its large remnant polarization[1~4]. Such materials with thin film form may provide for significant potential applications in future. Several papers have reported that large remnant polarization (P_r) is found in $BiFeO_3$ thin films derived from physical methods, e. g., PLD. However, no large value of P_r is observed in $BiFeO_3$ thin films from a chemical solution method[5]. Poor crystallization quality of the films and large leakage currents are considered to be responsible for the small P_r. Comparing with other ferroelectric materials, e. g., PZT, BST, $BiFeO_3$ has a much larger coercive electric field (E_c)[1,4], which imposes much more strict limitations

Received date: 2006-02-13, **revised date**: 2006-08-15 **收稿日期**:2006-02-13, **修回日期**:2006-08-15

Foudantion Item: Supported by the National Natural Science Foundation of China (60371040) and The Foundation of Science and Technology Commission of Shanghai Municipality (03JC14076)

Biography: SUN Jing-Lan(1962-), female, Shanxi, China, professor of Shanghai Institute of Technical Physics. Research area is ferroelectric material and infrared devices.

on the leakage current of $BiFeO_3$ films. In this paper, the transport properties of $BiFeO_3$ thin films prepared on lanthium nickelate (LNO) coated strontium titanate (STO) substrates by a chemical solution deposition method are investigated.

1 Experimental procedure and results

The $BiFeO_3$ thin films were prepared on LNO coated $SrTiO_3$(100) substrates. LNO coated $SrTiO_3$ substrates were selected because of small lattice mismatch between them and $BiFeO_3$ with a quasi-perovskite structure. Two kinds of samples, namely A and B, were obtained with the same precursor solution but different aged time. Samples A were obtained with fresh precursor solution, while B was fabricated with the same precursor solution stored in ambient atmosphere for six months. Detailed fabrication process and structure characterization of the films can be found in Ref. [6] and [7]. The thickness of both kinds of samples is ~160nm. Pt top electrodes with an area of 1×10^{-4} cm^2 were sputtered onto the sample with a photolithographic method. Ferroelectric property was characterized with a RT66. The Keithley6517 was employed to measure the weak leakage current under dc voltage bias. The variation of the temperature of the samples was controlled with a MMR temperature variation stage with micro probes.

Fig. 1 shows the ferroelectric properties and current versus voltage of the two kinds of samples at 85K. It can be seen that the leakage current in samples A is one order higher than that in samples B. Both A and B show a distortion in the negative voltage range, which is caused by the leakage current (as will be discussed below). Note that the P_r of samples A is one order larger than that of B. To have a deep insight into the mechanism which gives rise to the leakage current, careful investigations of dc electrical transport properties of the samples were carried out in the temperature range from 80K to 300K.

Upon the dc bias to a capacitor consisting of insulating film, three parts of current can be observed, charging current, absorbing current and leakage current. Theoretically the former two parts will vanish after a sufficient long time of waiting. In samples A, a

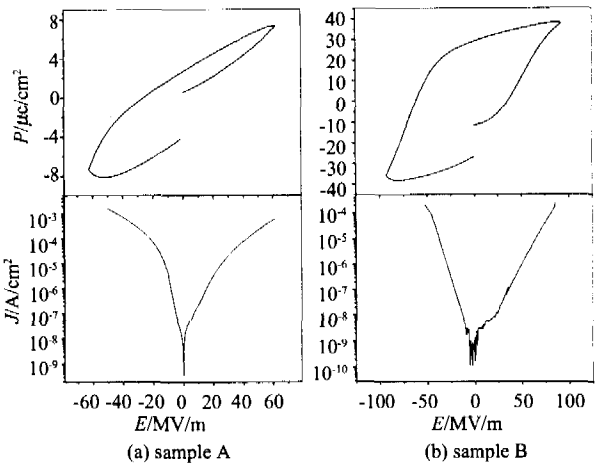

Fig. 1 Comparisons of ferroelectric and DC current versus voltage properties of the two kinds of samples at temperature of 85K.
图1 85K温度下两种样品的铁电和直流电流电压特性比较

steady state of leakage current can be obtained after a few seconds of the applying of the voltage. Fig. 2 shows a typical *I-V* curve of the samples at 85 K in a log-log scale. The inset magnifies the linear and exponential parts of *I-V* curve at 85K.

I-V measurement on the samples B is very difficult due to long waiting time to get a steady state. Meanwhile, electrical or thermal break down may happen after long stress time of dc bias. Thus current versus temperature under constant dc bias was measured in-

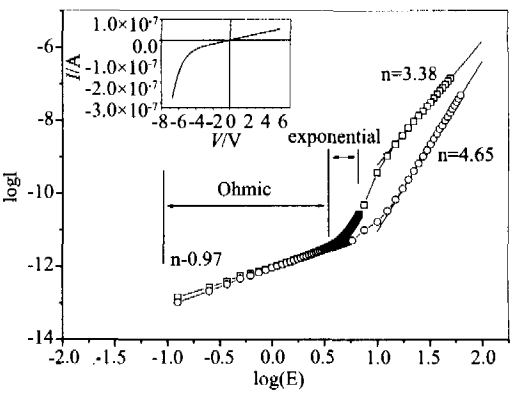

Fig. 2 *I-V* curve at 85K for sample A. Three regions; Ohmic, exponential, and power law dependence of current on voltage are observed. The curve represented by square is for negative voltage bias, circle for positive bias. Inset: *I-V* curve at low voltage bias
图2 样品A在85K的直流电流电压特性. 曲线分为欧姆型,指数型和幂指数型三个区域. 方块代表反向电压, 圆圈代表正向电压所测结果. 插图为低压下 *I-V* 曲线

stead of *I-V* curves. In this case, current under zero voltage bias was also measured to investigate the contribution of the thermal stimulated current[8]. In order to eliminate the pyroelectric current from the measured total current, data were taken with both increase and decrease of temperature at a rate of ±0.1K/s. Fig. 3 represents the variation of conductance with temperature under different dc bias. Each set of data was taken on a fresh sample (a capacitor) to avoid effects of voltage stress. The measurement was made for both positive and negative bias to check the effect of the observed asymmetry in the *I-V* curves.

For polycrystalline films, conductance obtained by a dc method consists of several transport processes, transport across grain boundaries, grains, and/or electrical interfaces[9]. To identify the probable transport process, the conductive tip AFM (CTAFM) morphology and resistance mapping of the films were carried out on samples B[10]. At low electric field, electric current was detected along the grain boundaries. At higher negative electric field, current transport across the whole grains. The current density kept at a low level under a positive electric filed. This rectifier behavior is consistent with the results of macroscopic dc measurement. A few conducting spots were found related to the second phase in the film as reported by H. Bea *et al*[11].

2 Discussions

2.1 Transport properties in samples A (with high leakage current)

Three regions in the curve of voltage dependence of current, Ohmic, exponential, and power law, were observed in this kind of samples (see Fig. 2). As shown in inset of Fig. 2, the *I-V* curve shows a rectifier characteristic at low voltage bias. Because of the deficiency of A-site atoms in an ABO_3 perovskite-structure film, the film is a p-type material. Schottky junction formed when platinum was used as electrodes[12]. Comparing the *I-V* results with the hysteresis loops of the samples, it can be concluded that the distortion in the PE curve is resulted from large leakage currents.

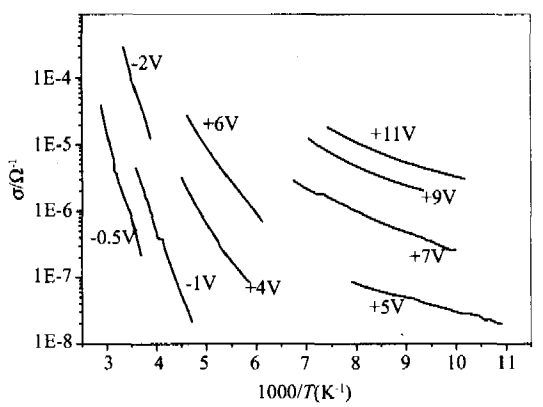

Fig. 3 Arrehenius plot of the temperature dependence of the conductance for samples B

图 3　样品 B 的电导随温度变化的 Arrehenius 图

2.2 Transport properties in samples B (with low leakage current)

There are several conductance mechanisms to explain the electrical transport in an insulating thin film[13]. A common feature is the exponential dependence of conductance on the temperature,

$$\sigma \propto A\exp\left\{-\frac{q}{k_B T}[\varphi-\beta]\right\} = A\exp\left\{-\frac{q}{k_B T}\alpha\right\} \quad , \quad (1)$$

where $\alpha = \varphi - \beta$, A is a constant independent or weekly dependent on the temperature, φ is the Schottky barrier or the defect energy level related to the conduction band of the material, and β is the lowering of the barrier by applied voltage,

$$\beta = \sqrt{qE/\pi\varepsilon_r\varepsilon_o} = \frac{1}{d}\sqrt{qS/\pi}\sqrt{V/C} \quad , \quad (2)$$

for Frenkel-Poole emission, and half of this value for Schottky emission, where E is the applied electric field, ε the dielectric constant, d the thickness of the film, S the area of the top electrodes, C the capacitance value of the capacitor, and V is the applied voltage. Thus by plotting the slope of the curves in Fig. 3 versus the square root of the applied electric field for each curve, the coefficient can be obtained experimentally. However, the situation in ferroelectric material is complicated by the fact that dielectric constant varies with both temperature and applied voltage. From dielectric measurement, it is found that the modulation of capacitance by applied voltage can be neglected. The capacitance changes by 20% from room temperature to 70K. Using an average value of the capacitance in the corresponding range of temperature for each data set in Fig. 3, the dependence of the slope for the curves in Fig. 3 on $\sqrt{V/C}$ can be obtained. The results are shown in Fig. 4. Two lines with distinct slopes were fitted to the

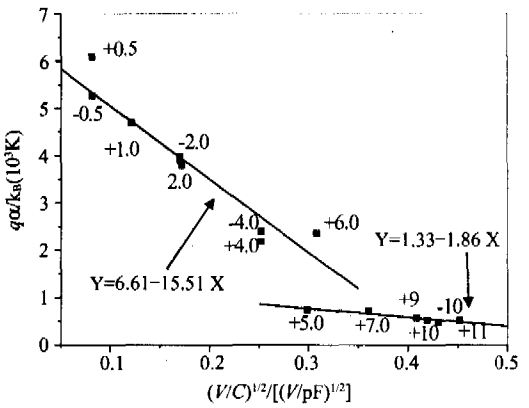

Fig. 4 The slope of curves in Fig. 3 versus $\sqrt{V/C}$. Solid lines are linear fitting to the data. The number near each date indicates the voltage at which the conductance was measured

图4 图3中曲线的斜率随$\sqrt{V/C}$的变化. 实线为拟合的直线. 实验点附近数据为测电导时外加的偏压值

low and high electric field regions, indicating different transport mechanism dominant in these two regions. For the lower field region, the energy barrier was 0.57eV, which is a reasonable value for the energy barrier at Pt/ $BiFeO_3$ interface or a carrier trap center in the insulator. However the slope is one order larger than the value for Schottky emission or Frenkel-Poole models. Fitting the line to the high electric field region results in an activation energy of 0.12eV. The slope of the line is in agreement with Frenkel-Poole model.

Comparing the above results with that of CTAFM, the fitting parameters in the low electric field should be adequate to describe transport across the $BiFeO_3$ grain boundaries. Since there are not any theory models available, further investigations need to be done about this issue.

3 Conclusion

The electrical transport mechanisms for chemical solution deposition derived $BiFeO_3$ thin films with high and low leakage current were studied. The samples with large leakage current showed a semiconductor like behavior. The low resistance prevented poling of the samples, which lead to a much smaller P_r. In high resistance thin films, the leakage current was along the grain boundaries at low electric fields. At high electric field the current transport across the whole grains. The process can be described by the Frenkel-Poole model.

REFERENCES

[1] Wang J, Neaton B, Zhang H, *et al.* Epitaxial $BiFeO_3$ multiferroic thin film heterostructures [J]. *Science*, 2003, **299**: 1719—1722.

[2] Yun K Y, Noda M, Okuyama M. Prominent ferroelectricity of $BiFeO_3$ thin films prepared by pulsed-laser deposition [J]. *Appl. Phys. Lett.*, 2003, **83**: 3981—3983.

[3] Neaton J B, Ederer C, Waghmare U V, *et al.* First-principles study of the spontaneous polarization in multiferroic $BiFeO_3$ [J]. *Phys. Rev. B.*, 2005, **71**: 014113.

[4] Yi-Hsien Lee, Jenn-Ming Wu, Yu-Lun Chueh, *et al.* Low-temperature growth and interface characterization of $BiFeO_3$ thin films with reduced leakage current [J]. *Appl. Phys. Lett.*, 2005, **87**: 172901.

[5] Iakovlev S, Solterbeck C H, Kuhnke M, *et al.* Multiferroic $BiFeO_3$ thin films processed via chemical solution deposition: Structural and electrical characterization [J]. *J. Appl. Phys.*, 2005, **97**: 094901.

[6] LI Ya-Wei, MENG Xiang-Jian, YU Jian, *et al.* Study on the preparation of $LaNiO_3$ thin films using chemical solution decomposition method [J]. *J. Infrared Millim. Waves* (李亚巍,孟祥建,于剑,等. 化学溶液分解法制备 LaNiO3 薄膜的研究. 红外与毫米波学报), 2003, **22**(4): 269—272.

[7] Li Y W, Sun J L, Chen J, *et al.* Preparation and characterization of $BiFeO_3$ thin. films grown on LaNiO3-coated SrTiO3 substrate by chemical solution deposition [J]. *J. Crys. Growth*, 2005, **285**: 595—599.

[8] Creswell R A, Perlman M M. Thermal currents from corona charged Mylar [J]. *J. Appl. Phys.*, 1970, **41**: 2365—2375.

[9] Iguchi E, Ueda K, and Jung W H. Conduction in $LaCoO_3$ by small-polaron hopping below room temperature [J]. *Phys. Rev.*, 1996, **B54**: 17431—17437.

[10] Houze F, Meyer R, Schneegans O, *et al.* Imaging the local electrical properties of metal surfaces by atomic force microscopy with conducting probes [J]. *Appl. Phys. Lett.*, 1996, **69**: 1975—1977.

[11] Bea H, Bibes M, Barthelemy A, *et al.* Influence of parasitic phases on the properties of $BiFeO_3$ epitaxial thin films [J]. *Appl. Phys. Lett.*, 2005, **87**: 072508.

[12] Scott J F. The physics of ferroelectric ceramic thin films for memory applications [J]. *Ferroelectrics Review*, 1998, **1**: 1—129.

[13] Sze. *Physics of Semiconductor Devices* [M]. New York: Willey, 1981.